Journal of Applied Electrochemistry **29**: 1359–1366, 1999.

The effect of ultrasonic frequency and intensity upon electrode kinetic parameters for the $Ag(S_2O_3)_2^{3-}/Ag$ redox couple

B. POLLET[1]*, J.P. LORIMER[1], S.S. PHULL[1], T.J. MASON[1], D.J. WALTON[1], J.Y. HIHN[2], V. LIGIER[2] and M. WÉRY[2]

[1]*School of Environmental and Physical Sciences, Coventry University, Priory Street, Coventry CV1 5FB, UK*

[2]*Laboratoire de Corrosion et Traitements de Surface, I.U.T. de Chimie 30, Avenue de l'Observatoire, 25009 Besançon, France*

*(*author for correspondence, e-mail: bpollet@aol.com)*

Received 23 September 1998; accepted in revised form 5 January 1999

Key words: photographic waste, silver electrodeposition, sonoelectrochemistry, Tafel equation

Abstract

This paper describes the effect of ultrasound on electrochemical parameters important in the removal of silver from photographic processing solutions. Decomposition voltages (obtained galvanostatically) and discharge potentials (obtained potentiostatically) for the reduction of the silver complex, $Ag(S_2O_3)_2^{3-}$ was studied in dilute aqueous $Na_2S_2O_3/NaHSO_3$ solution on stainless steel and carbon disc electrodes in both the absence and presence of ultrasound. Under silent conditions, silver deposition is the main reaction occurring at the electrode. Under sonication at 20 kHz and 500 kHz, the reduction wave shifts anodically with increasing ultrasonic intensity. Similarly, the discharge of hydrogen and oxygen shifts anodically and cathodically respectively with increasing ultrasonic power. The decrease in decomposition voltage in the presence of ultrasound is due to the combined effect of a decrease in anodic overpotential and an increase in cathodic overpotential.

1. Introduction

The primary sources of recoverable silver from photographic processing solutions are the 'wash' (dilute aqueous $Na_2S_2O_3$/ $NaHSO_3$) and the 'bleach-fix' solutions (dilute aqueous $Na_2S_2O_3/NaHSO_3$/NaFeEDTA) [1–4]. The various methods for recovering silver from such solutions are displacement by other metals (e.g., steel wool cartridges), ion-exchange (e.g., resins), electrolysis and bacterial digestion [2, 5, 6]. Currently, the most widely employed silver recovery method which meets regulatory limitations is electrolysis [6].

Only low concentrations of silver ion are present in the 'wash' solutions, the majority of which is bound up in complexes such as $Ag(S_2O_3)_2^{3-}$ and is deposited at the electrode by the following reaction [1]:

$$Ag(S_2O_3)_2^{3-} + e^- \longrightarrow Ag + 2\,S_2O_3^{2-} \quad (1)$$

Because the majority of the silver is in the form of negatively-charged complexes (e.g., $Ag(S_2O_3)_2^{3-}$), these tend to migrate away from the cathode. It was reported [3] that this shortage of argento-thiosulphate complexes at the electrode surface leads to the formation of a dark electrodeposit at the electrode, 'black' silver sulphide (Ag_2S) which is produced according to Equation 2 as follows [4]:

$$2\,Ag^+ + S^{2-} \longrightarrow Ag_2S \quad (2)$$

The sulphide ion produced from the decomposition of thiosulphate ions ($S_2O_3^{2-}$) reacts immediately with silver ions in solution depositing insoluble silver sulphide at the cathode (Equation 2) and thus preventing further electrodeposition of silver. However, if silver ions are kept at sufficient concentration around the cathode, this side reaction, called 'sulphiding', is minimized. This can be achieved by vigorous agitation of the solution: for example, by forced convection near the cathode.

Since 'wash' solutions have a low silver content (4–6 g dm^{-3}), the deposition is mainly diffusion controlled. Thus, to achieve a suitable space–time yield in the electrochemical cell, it is necessary to provide either high mass transfer conditions to the electrode or else to increase the electrode area [5, 6]. Conventionally, this is achieved either by using large surface area porous grains, rotating the cathode (the most common method used for the majority of commercial units), rotating the anodes (some minilab and large units) or by using static cathodes and anodes with agitation being provided by powerful pumps circulating the solution [6].

Another approach in enhancing the mass transfer is to apply ultrasonic vibration to the electrochemical cell.

The combination of ultrasound and electrochemistry is termed 'sonoelectrochemistry' [7, 8]; this is commonly used in a wide range of subject areas such as electrodeposition, electroplating, corrosion and electrochemical dissolution [7, 9].

Many of the observed effects of ultrasound in electrochemical processes can be explained by the enhancement in mass transport in diffusion-controlled processes. Sonication is believed to decrease the diffusion layer thickness thereby giving substantial increases in the limiting current. This may be due to the effects of cavitation together with microstreaming. Ultrasound can also affect the apparent electrode potential of a process and an early report on sonoelectrochemistry [10] showed that the overpotential of hydrogen evolution on a gold electrode immersed in water decreases upon sonication.

This paper reports the effect of ultrasonic frequencies and intensities on the irreversible $Ag(S_2O_3)_2^{3-}/Ag$($E^\circ = +0.017$ V vs SHE [11, 12]) redox couple by examining current–voltage curves as a means of identifying the important electrode kinetic parameters. It should be emphasized that this paper does not report conventional electrolysis of 'wash' solution. However, it was observed that, under silent conditions, silver deposition is the main cathodic reaction occurring during the electrolysis of 'wash' solution. This observation was evident from SEM–EDAX analysis of the electrodeposits which indicated that relatively pure silver was present in the deposit (a large silver peak was depicted and no sulphur peaks were apparent). Under sonication, it was observed that above 24 W cm^{-2} (20 kHz) some of the silver electrodeposit was unintentionally removed from the electrode. For all the ultrasonic intensities employed, the silver deposit was shiny and compact.

A detailed study of the morphology and amount of silver recovered is the subject of our current investigation and will be further discussed in a forthcoming paper.

2. Experimental details

Potentiostatic experiments were carried out using either a Pine RDE4 potentiostat linked to a JJ Instruments X–Y chart recorder or a Radiometer PGP201 potentiostat linked to a 486DX Viglen computer via a RS232C serial interface. Electrochemical software (VoltaMaster 1) was employed to control the Radiometer PGP201 potentiostat. All galvanostatic experiments were performed using a Thurlby (model PL320) d.c. voltage supplier (maximum current and voltage up to 200 mA and 5 V, respectively). The d.c. voltage supplier was fitted with a digital display for accurate current and potential measurements. Current was measured using a Fluke 8010A digital multimeter as an ammeter. Electrochemical experiments were performed using either a one-compartment cell, a three-compartment cell (Figure 1)

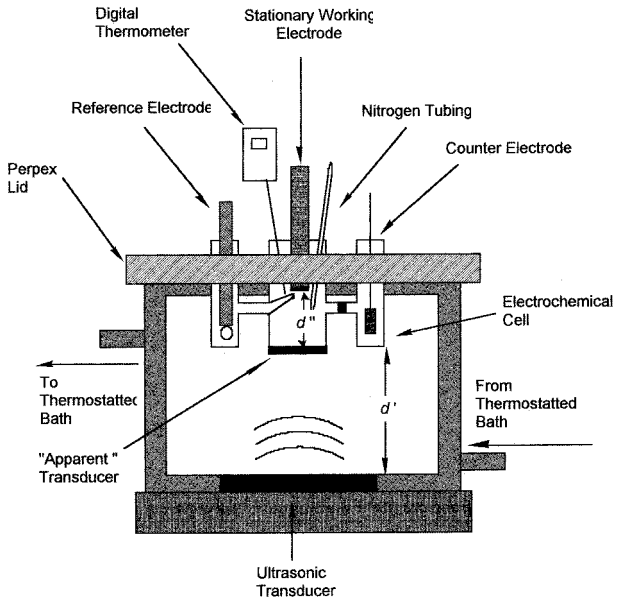

Fig. 1. A 500 kHz ultrasonic bath used for sonoelectrochemical experiments.

[13, 14] or a cell similar in design to that of Compton et al. [15] with the exception that the source of ultrasound (Sonics & Materials VC50 horn) was placed at the bottom of the electrochemical cell (Figure 2).

All electrochemical cells were placed in a Faraday cage. Temperature was regulated by either an electrical insulated stainless steel cooling coil (C) placed inside the electrochemical cell (Figure 2) or a cooling jacket (Figure 1) linked to a thermostatted bath operating at preset temperatures. Temperature of the electroanalyte

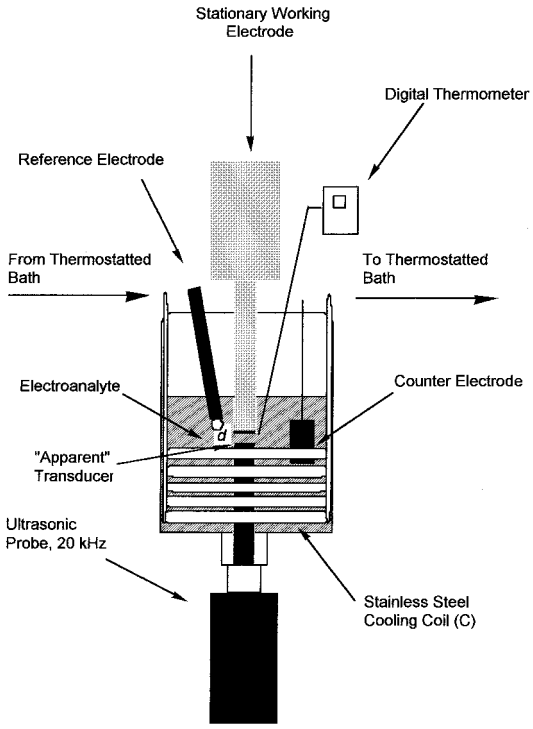

Fig. 2. Compton cell arrangement [16] with the exception of the ultrasonic source (Sonics & Materials VC50 probe) at the bottom.

was measured with a Fluke 51 digital thermometer fitted to a K-type thermocouple. The working electrodes were a 316 stainless steel and a carbon disc of similar dimensions (area 0.196 cm^2). A platinum flag electrode (1 cm^2) was used as the counter electrode. A saturated calomel electrode (SCE) was employed as the reference electrode. For the Compton cell arrangement, the distance between the ultrasonic probe and the working electrode was approximately 2 mm (d, Figure 2). For the three-compartment cell arrangement, the distance between the base of the cell and the transducer was approximately 5 cm (d', Figure 1) and the distance between the working electrode and the base of the cell was approximately 1 cm (d'', Figure 1). All carbon disc electrodes were manufactured by Oxford Electrodes and electrochemically cleaned by cycling in 1.0 M sulphuric acid from 0 to −1.0 V vs SCE at 100 mV s^{-1} for 20 min and held at −1.0 V vs SCE for 2 min. The carbon electrodes were then washed with distilled water and oven dried overnight (110 °C). All 316 stainless steel disc electrodes were placed in a beaker of 0.5 M sulphuric acid for 10 min. The electrodes were removed and washed with high quality MilliQ water before being polished with grinding paper (Buelher-Met, P600) and sequentially with 25 μm down to 0.3 μm alumina oxide until a mirror finish. The counter platinum electrode was electrochemically cleaned by cycling in sulphuric acid (1.0 M) for 10 min.

All chemical reagents were of AnalaR grade or equivalent. Silver chloride (Aldrich, 99%, AR) was added to aqueous solutions of sodium thiosulphate (Fisons, AR) and sodium bisulphite (Fisons, AR) in deionized water to produce model photographic solutions which were deaerated by bubbling nitrogen for 20 min prior to experiments. All silver deposits were analysed by SEM–EDAX. Ultrasound was provided from either a 20 kHz probe (Sonics & Materials VC50, 0.17 cm^2, maximum power 43 W cm^{-2}) or a 500 kHz bath (Undatim Ultrasonics Sonoreactor, maximum power 0.2 W cm^{-2}). Ultrasonic powers were determined calorimetrically [16, 17] and ultrasonic intensities were quoted as Wcm^{-2}.

3. Results and discussion

3.1. *Effect of ultrasound on decomposition voltage and discharge potential of silver in thiosulphate solution*

Galvanostatic experiments were conducted on 4 g dm^{-3} of Ag (as AgCl) in dilute aqueous $Na_2S_2O_3/NaHSO_3$ solution ('wash' solution) using a carbon (C) electrode as the anode and a stainless steel (SS) electrode as the cathode in the absence and in the presence of ultrasound (20 and 500 kHz) at various ultrasonic intensities and at 298 ± 1 K. In these experiments, the ultrasonic horn (Sonics & Materials VC50) was placed between the anode and the cathode in a one-compartment cell. For the 500 kHz experiments, the one-compartment cell was placed directly into the 500 kHz ultrasonic bath (Undatim). Voltage was applied across the electrolytic cell using a d.c. voltage supplier and increased from 0 to 4 V in steps of 0.2 V while the current was monitored. Cell decomposition voltages (E_D) were determined by extrapolating the rising part of the current–voltage curve to the x-axis [18].

Figure 3 shows the current–voltage curves of the 'wash' solution in the absence and presence of ultrasound at two frequencies (20 and 500 kHz), three ultrasonic intensities (0.2, 24 and 43 W cm^{-2}) and at 298 ± 1 K. The decomposition voltages obtained from Figure 3 were plotted against the square root of the ultrasonic intensity (Figure 4) to yield a reasonably good linear relationship. The Figure demonstrates that as the ultrasonic intensity is increased there is a significant decrease in the decomposition voltage. For example, at a maximum ultrasonic intensity (43 W cm^{-2}, 20 kHz), the decrease in decomposition voltage is of the order of 10% when compared to the silent condition. In other words, there is a maximum average shift of the decomposition voltage of approximately 155 mV. The Figure also indicates that the decomposition voltage does not vary significantly with ultrasonic frequency but rather with ultrasonic intensity. This substantiates other previous observations [13, 14].

To examine whether this decrease in decomposition voltage was due to an overall shift in discharge potential (i.e., $E_D = E_{dc} - E_{da}$), the variation of the individual anodic and cathodic discharge potentials obtained under conditions of insonation was investigated. For this purpose, the reduction of the silver cation together with the oxidative evolution of oxygen were studied in dilute $Na_2S_2O_3/NaHSO_3$ solution. Experiments were per-

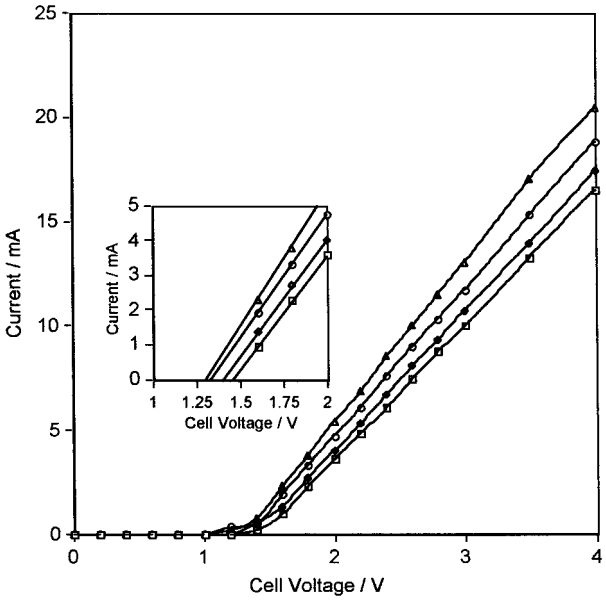

Fig. 3. Current–voltage curves of silver in $Na_2S_2O_3/NaHSO_3$ solution in the absence and presence of ultrasound (20 and 500 kHz) at various ultrasonic intensities and at 298 ± 1 K. Key: (□) silent, (◇) 0.2 W cm^{-2} (500 kH_3), (○) 24 W cm^{-2} (20 kH_3) and (△) 43 W cm^{-2} (20 kH_3).

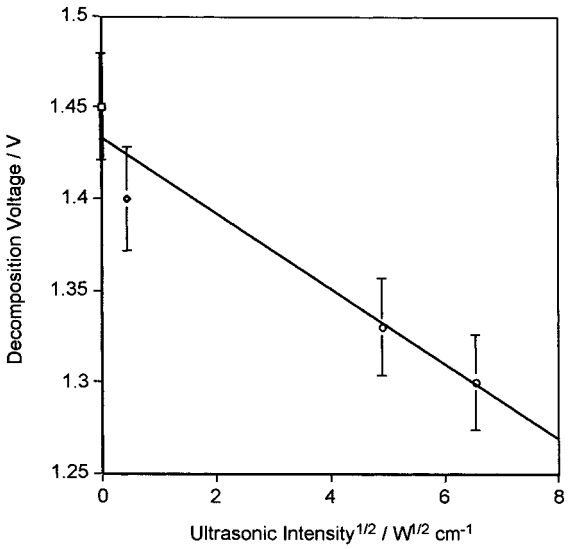

Fig. 4. Decomposition voltages plotted against square root of ultrasonic intensity at two ultrasonic frequencies and at 298 ± 1 K for the 'wash' solution. Key: (□) silent, (◇) 500 kH_3 and (○) 20 kH_3.

formed potentiostatically using the two types of electrode material [SS and C] in 4 g dm^{-3} Ag in dilute aqueous $Na_2S_2O_3/NaHSO_3$ solution in the absence and presence of ultrasound (20 and 500 kHz) at various ultrasonic intensities and at 298 ± 1 K. For such experiments, the three-compartment cell (Figure 1) was employed. The working electrode potential was varied from 0 to −1.4 V vs SCE for cathodic scans and from 0 to +1.4 V vs SCE for anodic scans at 5 mV s^{-1} scan rate. The anodic (E_{da}) and cathodic (E_{dc}) discharge potentials were obtained by extrapolating the rising parts of the polarization curve to the *x*-axis [18].

Figure 5 shows the anodic and cathodic polarization curves of our electrolyte on the carbon and stainless steel electrodes respectively in the absence and presence of ultrasound (20 kHz). The anodic and cathodic parts of the voltammogram correspond to the evolution of oxygen on carbon and the deposition of silver on stainless steel respectively. The more cathodic part of the curve also shows the evolution of hydrogen on a silver covered stainless steel electrode. The Figure shows that the silver, oxygen and hydrogen discharge potentials are influenced by sonication, that is, both silver and hydrogen discharge potentials shift anodically whereas the oxygen discharge potential shifts cathodically.

The cathodic part of Figure 5 shows improved mass-transport in that a sigmoidal shaped voltammogram is obtained for the reduction of silver in the presence of ultrasound (reduction wave, C). The existence of this plateau is thought to be due to a decrease in the diffusion layer thickness caused by jetting together with microstreaming [7, 8]. Transport rates 10^2–10^3 times higher than those of other hydrodynamics techniques have been shown to be easily attainable in experiments conducted in the presence of ultrasound [13].

Figure 6 shows a plot of oxygen anodic discharge potential vs the square root of the ultrasonic intensity at two ultrasonic frequencies (20 and 500 kHz) and at 298 ± 1 K. The Figure shows an approximately linear relationship between the anodic discharge potential and the square root of the ultrasonic intensity. It is interesting to note that at 20 kHz a maximum average shift of

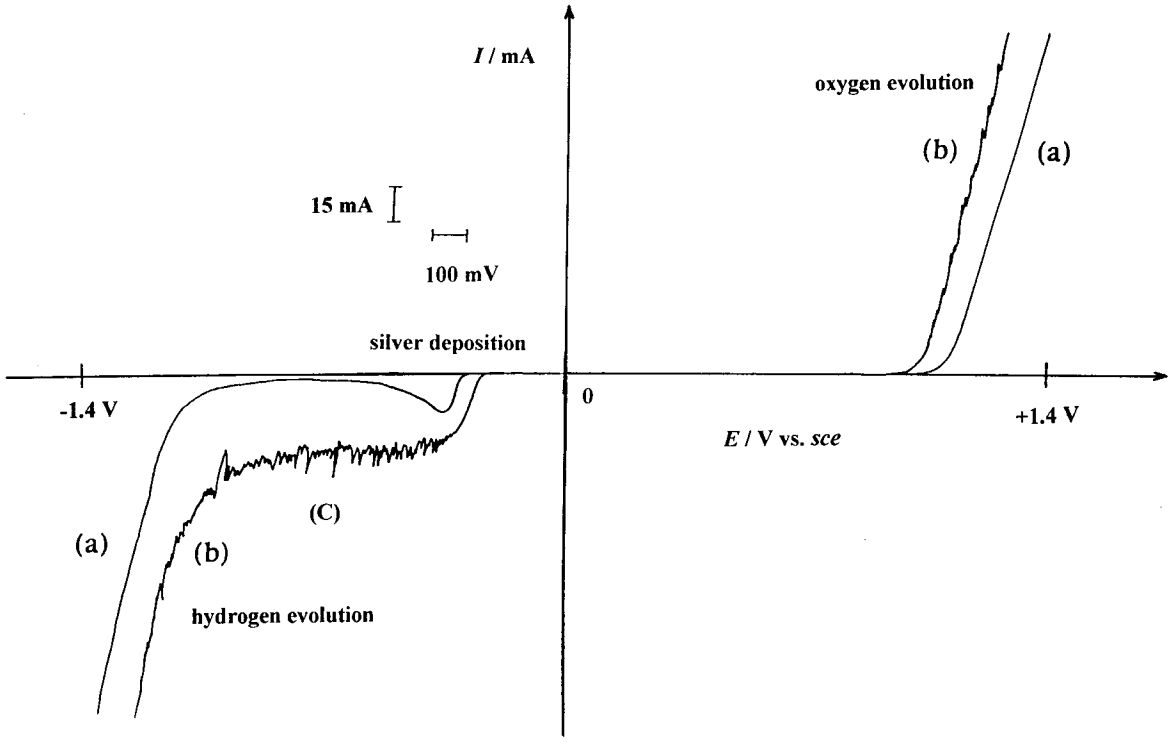

Fig. 5. Polarization curves of 4 g dm^{-3} of silver in $Na_2S_2O_3/NaHSO_3$ solution on stainless steel and carbon disc electrodes (area 0.196 cm^2) in the (a) absence and (b) presence of ultrasound (VC50, 20 kHz, 43 W cm^{-2}) at 298 ± 1 K.

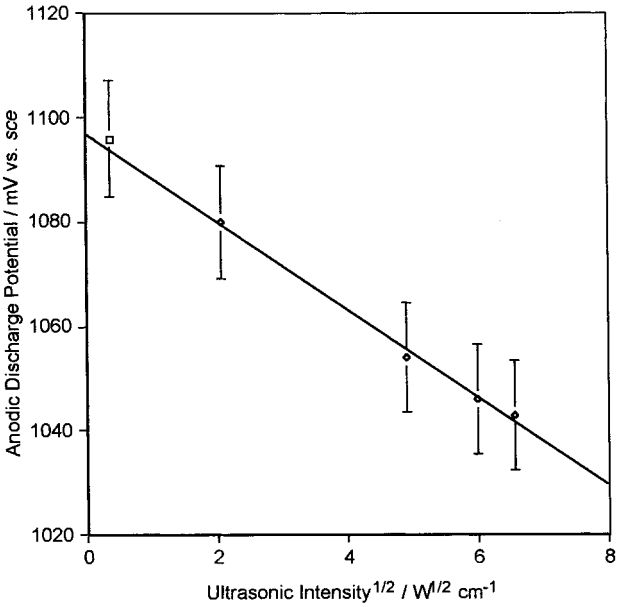

Fig. 6. Anodic discharge potential of oxygen in 'wash' solution plotted against square root of ultrasonic intensity at two ultrasonic frequencies and at 298 ± 1 K. Key: (□) 500 kH_3 and (◇) 20 kH_3.

the anodic potential of approximately −75 mV is observed. In other words, the oxygen discharge potential shifts cathodically under insonation. Having observed galvanostatically that the total shift in the decomposition voltage is decreased by 155 mV, and that the contribution from the anodic discharge potential is −75 mV, one may propose that the cathodic discharge potential should be shifted by +80 mV, that is, anodically in the same range of ultrasonic power employed.

To show that this is true, the cathodic discharge potential was plotted against the square root of the ultrasonic intensity (Figure 7). The Figure shows an approximate linear relationship with a maximum average shift of approximately +70 mV. This result is in agreement with that deduced using values of the decomposition voltage (+80 mV). It is interesting to note that the magnitude in potential shift is similar for the deposition of silver and the evolution of oxygen on different electrode surfaces. This may be coincidental or else may suggest that the effect of ultrasound on the potential depends less on the electrolytic process occurring at the electrode surface but more on the sonochemical effect. It has been suggested [9, 19, 20] that these shifts in potentials are linked to overpotential phenomena and may have several possible origins.

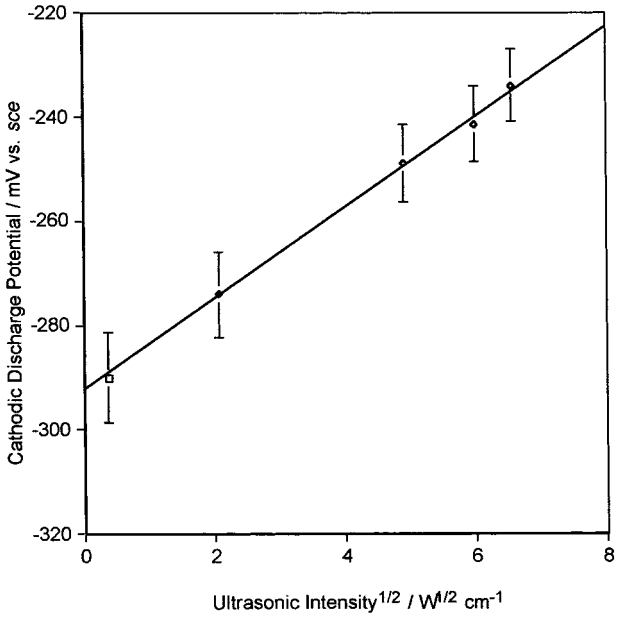

Fig. 7. Cathodic discharge potential of oxygen in 'wash' solution plotted against square root of ultrasonic intensity at two ultrasonic frequencies and at 298 ± 1 K. Key: (□) 500 kH_3 and (◇) 20 kH_3.

3.2. *Effect of ultrasound on overpotential*

Figure 8 shows hydrogen overpotential against log (i) at two ultrasonic frequencies (20 and 500 kHz) and three intensities (0.2, 24 and 43 W cm^{-2}) on a silver covered stainless steel electrode. The Figure shows that ultrasound decreases the hydrogen overpotential below that found under natural convection. For example, at a current density of 6.92×10^{-4} A cm^{-2} (log $i = -3.16$), cathodic overpotentials of about −0.1 and 0.02 V vs SCE were obtained in the absence and presence of 43 W cm^{-2} of ultrasound (20 kHz), respectively (i.e., a decrease of approximately +80 mV required for discharge). This shift is in good agreement with that obtained with discharge potentials. Thus, if it assumed that $\eta = E_{app} - E_{rev}$, it might be suggested that the shift in potential is solely due to overpotential rather than in the reversible (equilibrium) potential.

Further, the decrease in overpotential occurs without any appreciable change in the Tafel slope (163 mV). This result suggests that the electron-transfer coefficient, α, is not affected by sonication. In other words,

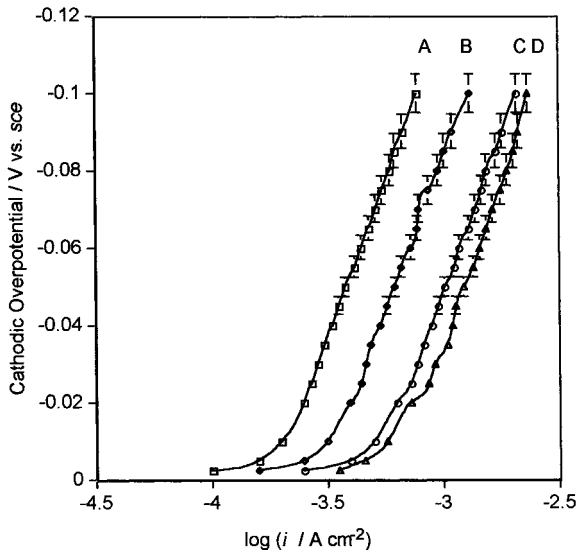

Fig. 8. The effect of ultrasound upon Tafel plots for the evolution of hydrogen on silver covered stainless steel electrode at 298 ± 1 K. Key: (A, □) silent, (B, ◇) 0.2 W cm^{-2} (500 kH_3), (C, ○) 24 W cm^{-2} (20 kH_3) and (D, △) 43 W cm^{-2} (20 kH_3).

partitioning of the change in the potential energy of the system between the forward and reverse reactions is not affected by insonation. However, a modification of the Tafel plots is clearly evident when one compares the exchange current density obtained in the absence and presence of ultrasound. Since the Tafel equation is given by $\eta = a + b \log i_{net}$ where $a = 2.3\,RT \log i_o/(\alpha nF)$ and $b = -2.3\,RT/(\alpha nF)$ (= 163 mV), the decrease in the a values (i.e., intercepts) is seen to be influenced by ultrasonic intensity. Since the electron-transfer coefficient, α, appears not to be affected by sonication, this change in a is due mainly to an increase in exchange current density, an observation corroborated by other workers [21, 22]. For the present system, i_o, at the maximum ultrasonic intensity of 43 W cm^{-2} is found to be 0.62 mA cm^{-2} whereas under silent conditions the value is 0.19 mA cm^{-2} i.e., a threefold increase on the application of ultrasound. Since the exchange current density is proportional to the apparent heterogeneous rate constant [23], this finding suggests that the apparent heterogeneous rate constant is increased by approximately 200% in the presence of ultrasound.

It is known [23, 24] that the increase in the apparent heterogeneous rate constant, k_o, is due to either changes in electrode surface composition or changes in temperature. Since the macroscopic temperature of the bulk does not change during sonication, the increase in the apparent heterogeneous rate constant must be due to either a modification of the electrode surface composition or an increase in the microscopic temperature within the diffusion layer due to the implosion of high-energy cavitation bubbles. This could explain the increase in limiting current density [25] and the shift in half-wave potentials [26].

Two mechanisms [20] have been proposed to explain the decrease in overpotential under conditions where concentration polarization involving the electrolyte should be negligible.

The first is that ultrasonically-produced cavitation modifies the surface of the electrode, for example, by changing the number of sites available for the adsorption of hydrogen on the electrode surface. The erosive action associated with the implosion of high-energy cavitation bubbles should produce a new electrode surface continuously and at the same time promote the removal of adsorbed impurities on the electrode surface. Also, it is known that the apparent heterogeneous rate constant depends on the overpotential [23] which in turn depends on the active sites available on the electrode surface for the electron-transfer. Since a decrease in overpotential leads to an increase in active sites, it may be speculated that, on application of ultrasound, the electron-transfer becomes more facile.

The second mechanism proposed to explain a part of the decrease in hydrogen overpotential produced by ultrasound involves the degassing effects associated with microstreaming together with cavitation. It has been shown [9, 19, 20] that the solution adjacent to the electrode surface is supersaturated with molecular hydrogen (because of the low solubility of molecular hydrogen in aqueous solutions) leading to the so-called 'bubble overpotential'. It has been suggested [27] that acoustic streaming and cavitation could help degas the solution immediately adjacent to the electrode, thus, decreasing and even eliminating the 'bubble overpotential'.

Figure 9 shows the effect of ultrasonic intensity on silver overpotential on stainless steel electrode in $Na_2S_2O_3/NaHSO_3$ solution. Similar to hydrogen (Figure 8), it was found that the Tafel slope did not increase significantly with ultrasonic intensity (43 W cm^{-2}, $b = 118.6$ mV) when compared to silent conditions ($b = 118$ mV). It was interesting to note that at a high current density (i.e., log $i = 1.38$; $i = 23.98$ mA cm^{-2}) the silver overpotential on stainless steel was reduced by approximately 70 mV without any appreciable change in the Tafel slope. It was also found that at maximum power (43 Wcm^{-2}) the exchange current density ($i_o = 11.72$ mA cm^{-2}) was increased by threefold compared with silent conditions ($i_o = 3.71$ mA cm^{-2}). It is possible to explain this result as follows:

(i) It is well-known that when ultrasound is transmitted through a liquid, efficient stirring and cavitation occur in the bulk solution and near the electrode surface. This leads to an increase in the movement of ions across the diffusion layer and their subsequent discharge [20] and hence a decrease in concentration overpotential. This also leads to a decrease in nucleation overpotential [10]. It has been shown that ultrasound affects the surface morphology of many metal electrodeposits due to highly efficient stirring caused by acoustic streaming, and also that this decrease in overpotential is due to formation of nucleation sites at the electrode surface caused by the implosion of cavitation bubbles [7, 10].

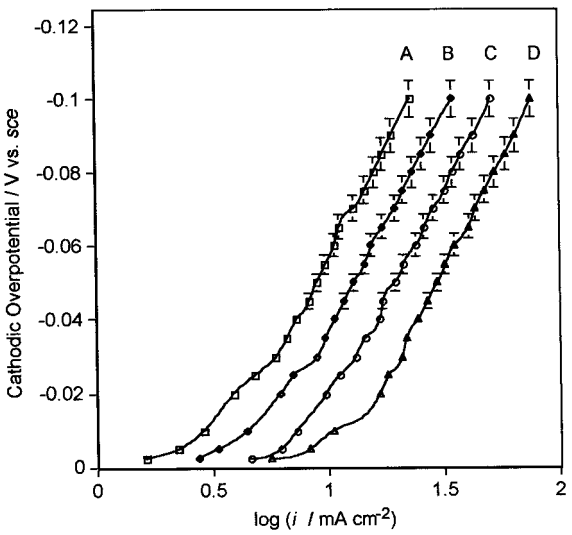

Fig. 9. The effect of ultrasound upon Tafel plots for the deposition of silver on stainless steel electrode at 298 ± 1 K. Key: (A, □) silent, (B, ◇) 0.2 W cm^{-2} (500 kH$_3$), (C, ○) 24 W cm^{-2} (20 kH$_3$) and (D, △) 43 W cm^{-2} (20 kH$_3$).

(ii) It is also known that increasing the effective area of an electrode surface causes a decrease in overpotential as is shown by a comparison of typical values for smooth platinum and finely divided platinum black electrodes [18]. Since ultrasound is known to cause pitting of metal surfaces, this is a possible explanation for the decrease in overpotential [9]. However, this seems not to apply in this case since the silver discharge potential under silent conditions at the stainless steel electrode is approximately the same before ($E_{dc,b}$) and after ($E_{dc,a}$) exposure of the electrode to ultrasound (43 W cm^{-2}, 20 kHz), that is, $\Delta E_{dc} = E_{dc,a} - E_{dc,b} = +6$ mV, and the electrode used in the study was polished between each run.

(iii) Temperature has an obvious influence on electrode kinetics [23] and the potential E is known to be temperature-dependent. Over the range 298–323 K, a 7 mV positive shift was observed under silent conditions (Figure 10) compared with a 75 mV positive shift in the presence of ultrasound (20 kHz, 43 W cm^{-2}). Since ultrasonic irradiation leads to a temperature increase in a medium, it is important to establish whether a decrease in potential under sonication is due to bulk temperature increase. Comparison of the silver cathodic discharge potential at various bulk temperatures (Figure 10) with those in the presence of 20 kHz ultrasound (Figure 7, 43 W cm^{-2}) (assuming linearity between E_{dc} and T), makes it possible to deduce an 'apparent' bulk temperature in the presence of 43 W cm^{-2}. In order to achieve this 75 mV shift in potential, the bulk temperature under purely thermal conditions would have to be approximately 500 K. A similar value was deduced for the oxygen anodic discharge potential. However, the temperature of the bulk solution never rose above 298 ± 1 K during the ultrasonic runs. A similar 'apparent' bulk temperature has been previously deduced to be approximately 400 K [13].

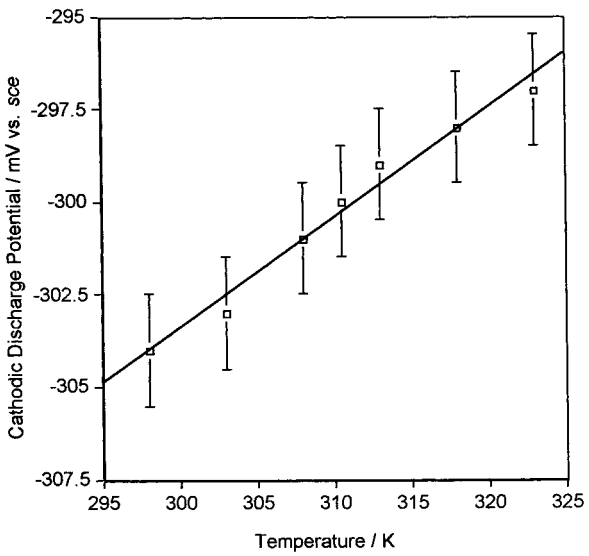

Fig. 10. Dependency of cathodic discharge potential of silver from 'wash' solution with temperature.

One possible explanation of this shift in potential is an increase in the local temperature within the diffusion layer rather than an increase in bulk temperature. If it is assumed that the maximum temperature on bubble collapse can be represented by the modified Noltingk and Neppiras expression [14, 28], that is,

$$T_{max} \approx \frac{T_o(\gamma - 1)\left[P_h + (2\rho c I^{1/2})\right]}{P_v} \quad (3)$$

and provided that ρ, c and E_{rev} (+0.452 V vs SCE) can be assumed to be 'constant' in a cavitating medium, then for a given system η_c should be a function of $I^{1/2}$ (Equation 4, Figure 11)

$$T_{max} = A + BI^{1/2} \quad (4)$$

In the above T_o is the ambient temperature, γ is the ratio of the specific heats of the gas (or gas vapour) mixture, P_v is the vapour pressure of the liquid, P_h is the ambient hydrostatic pressure, ρ is the density of the medium, c is the velocity of sound in that medium and I is the ultrasonic intensity.

A similar trend to that found for the cathodic overpotential (Figure 11) was also obtained for the anodic overpotential.

4. Conclusions

It was shown that, in our conditions, the decomposition voltage decreases with increasing ultrasonic intensity

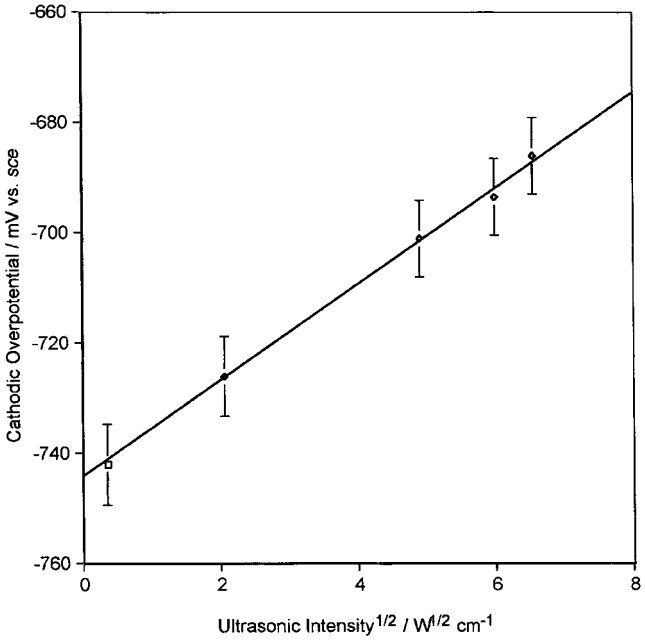

Fig. 11. Cathodic overpotential of silver in $Na_2S_2O_3/NaHSO_3$ solution plotted against square root of ultrasonic intensity at two ultrasonic frequencies and at 298 ± 1 K. Key: (□) 500 kH_3 and (◇) 20 kH_3.

due to an anodic and a cathodic potential shift of approximately −75 mV and +70 mV, respectively. This gives an overall potential shift of approximately 145 mV (if $E_D = E_{dc} - E_{da}$) which compares favourably with the decomposition voltage shift (155 mV) obtained experimentally across the whole cell in the presence of ultrasound.

It appears that this shift in discharge potential might be due to a change in the overpotential rather than in the reversible potential. The increase in cathodic discharge potential and the decrease in anodic potential may not be due to an increase of bulk temperature but might rather be attributed to an increase of local (microscopic) temperature differentials within the diffusion layer caused by the implosion of cavitation bubbles or some other effect of greatly enhanced hydrodynamic motions. However, the main factor responsible for the change in the electrode overpotential during insonation appears to be the removal of ions from the diffusion layer caused by the acoustic streaming and the disruption of the diffusion layer by cavitation effect.

Ultrasound is useful as a means of obtaining microscopically fresh surfaces. The ability of sonication through cavitation to erode metal surfaces provides a constantly renewed surface. This may be useful in studies on overpotential phenomena to separate out the contributions from different surface processes and associated diffusional effects.

Acknowledgements

The authors wish to thank Professor R.G. Compton for the loan of the sonoelectrochemical cell and Professor D. Feakins for helpful discussions.

References

1. A.C. Cooley and T.J. Dagon, *J. Appl. Photogr. Eng.* **2** (1976) 36.
2. N. Sathaiyan, P. Adaikkalam and S. Visvanathan, *J. Photogr. Sci.* **41** (1993) 146.
3. A.C. Cooley and D. Vacco, *J. Imaging Science and Technology* **37** (1993) 603.
4. A.C. Cooley, *J. Imaging Sci. Technol.* **37** (1993) 374.
5. A. Storck and F. Coeuret, *Eléments de Génie Electrochimique*, Lavoisier, Techniques et Documentation, Paris (1993) p. 49.
6. D. Pletcher and F.C. Walsh, *Industrial Electrochemistry* (Blackie Academic and Professional, Glasgow, 1993) p. 24.
7. D.J. Walton and S.S. Phull, In: T.J. Mason (ed.) *Advances in Sonochemistry*, vol. 4, (JAI Press, London, 1996) p. 205.
8. R.G. Compton, J.C. Eklund, F. Marken, T.O. Rebbitt, R.P. Akkermans and D.N. Waller, *Electrochim. Acta* **42** (1997) 2919.
9. R. Walker, *in Advances in Sonochemistry* (ed. by T.J. Mason) vol. 3, (JAI Press, London, 1993) p. 125.
10. N. Moriguchi, *J. Chem. Soc. Japan* **55** (1934) 749.
11. G. Milazzo and S. Caroli, *Tables of Standard Electrode Potentials*, (J. Wiley & Sons, New York, 1978) p. 43.
12. J.M. Grau and J.M. Bisang, *J. Chem. Tech. Biotechnol.* **53** (1992) 105.
13. J.P. Lorimer, B. Pollet, S.S. Phull, T.J. Mason, D.J. Walton and U. Geissler, *Electrochim. Acta* **41** (1996) 2737.
14. J.P. Lorimer, B. Pollet, S.S. Phull, T.J. Mason and D.J. Walton, *Electrochim. Acta* **43** (1998) 449.
15. J.C. Eklund, F. Marken, D.N. Waller and R.G. Compton, *Electrochim. Acta* **41** (1996) 1541.
16. T.J. Mason, J.P. Lorimer and D.M. Bates, *Ultrasonics* **30** (1992) 40.
17. M.A. Margulis and A.N. Mal'tsev, *Russ. J. Phys. Chem.* **43** (1969) 592.
18. S. Glasstone and D. Lewis, *Elements of Physical Chemistry*, Macmillan, London (1960) p. 492.
19. F. Cataldo, *J. Electroanal. Chem.* **332** (1992) 325.
20. E. Yeager, T.S. Oey and F. Hovorka, *J. Phys. Chem.* **57** (1953) 268.
21. H. Zhang and L.A. Coury (Jr), *Anal. Chem.* **65** (1993) 1552.
22. F. Marken, J.C. Eklund and R.G. Compton *J. Electroanal. Chem.* **395** (1995) 335.
23. A.J. Bard and L.R. Faulkner, *Electrochemical Methods*, J. Wiley & Sons, New York (1980) p. 101.
24. Southampton Electrochemistry Group, *Instrumental Methods in Electrochemistry* (Ellis Horwood, Chichester, UK, 1990) p. 77.
25. C.R.S. Hagan and L.A. Coury, *Anal. Chem.* **66** (1994) 399.
26. R.G. Compton, J.C. Eklund and S.D. Page, *J. Phys. Chem.* **99** (1995) 4211.
27. D.J. Walton, S.S. Phull, A. Chyla, J.P. Lorimer, T.J. Mason, L.D. Burke, M. Murphy, R.G. Compton, J.C. Eklund and S.D. Page, *J. Appl. Electrochem.* **25** (1995) 1083.
28. T.J. Mason and J.P. Lorimer, 1988. *Sonochemistry, Theory, Applications and Uses of Ultrasound in Chemistry* (Ellis Horwood, Chichester, UK, 1988) p. 43.